Damping of the double giant dipole resonance

Nguyen Dinh Dang,[1,*] Kosai Tanabe,[2] and Akito Arima[1,3]
[1]*RI-beam Factory Project Office, The Institute of Physical and Chemical Research, 2-1 Hirosawa, Wako, Saitama 351-0198, Japan*
[2]*Department of Physics, Saitama University, 255 Shimo-Okubo, Urawa, Saitama 338-8570, Japan*
[3]*Ministry of Education & Science and Technology, Chiyoda-ku, Kasumigazeki 3-2-2, Tokyo, Japan*
(Received 22 October 1998)

A microscopic approach is proposed to the damping of the double giant dipole resonance (DGDR). The double-time Green's function method is used to derive a closed set of coupled equations for the propagation of two-phonon excitation through the field of incoherent nucleon pairs. The analytical expressions for the width and energy shift of the DGDR are obtained. The numerical calculations are performed for ^{90}Zr, ^{90}Sn, and ^{208}Pb for several characteristics of the DGDR at zero as well as nonzero temperatures T. The results are found in reasonable agreement with existing experimental systematics for the width and energy of the DGDR. As compared to the estimation within the harmonic picture, the anharmonicity leads to a noticeable enhancement of the integrated photoabsorption cross section (IPACS) over the DGDR region. The DGDR width is found to increase sharply with increasing T at $T \leqslant 3$ MeV, but goes to a saturation at $T > 3$ MeV. The harmonic limit for the DGDR width is restored already at $T \geqslant 1.5$ MeV. It is shown that the IPACS of the DGDR can also be enhanced compared to its harmonic value if it is built on a hot GDR. [S0556-2813(99)03706-1]

PACS number(s): 24.30.Cz, 24.10.Pa, 25.75.−q

I. INTRODUCTION

The study of multiphonon excitations in nuclei has attracted considerable interest during the past years [1]. An unambiguous signature of the double giant dipole resonance (DGDR) has been obtained in pion-induced charge exchange reactions [2] and relativistic heavy-ion reactions via Coulomb excitation [3,4]. Since a giant resonance is a collective excitation, which can be well described by the first oscillator quantum (phonon), a multiphonon excitation can be interpreted as a giant resonance built on top of other giant resonances. This leads to the harmonic picture, in which a multiphonon excitation is considered as composed of independent phonons. In the harmonic limit the energy of a multiphonon state is just the sum of energies of the constituting single-phonon (boson) states. According to the golden rule, the width of the multiphonon resonance is also the sum of the individual widths of single-phonon resonances. This is valid when the spreading width of a single-phonon resonance is relatively small as compared to the energy range within which the level density and the coupling matrix elements can be considered approximately constant [5]. The decay of a single-phonon resonance can then be associated with a Lorentzian distribution [6]. In the strong coupling limit, where the shape of the single-phonon resonance approaches the Gaussian distribution, the width of the multiphonon resonance is the quadratic sum (rather than the sum) of the widths of single-phonon resonances [5,6].

In reality the main features of the observed DGDR can be summarized as follows.

(i) The energy E_{DGDR} of the DGDR is about twice as large compared to the giant dipole resonance (GDR): $E_{\mathrm{DGDR}} \simeq 2E_{\mathrm{GDR}}$, i.e., well described by the harmonic picture.

(ii) The observed width Γ_{DGDR} of the DGDR is in between $\sqrt{2}\Gamma_{\mathrm{GDR}}$ and $2\Gamma_{\mathrm{GDR}}$, where Γ_{GDR} is the GDR width.

(iii) The magnitude of the measured total electromagnetic excitation cross section is found to be enhanced up to more than three times as large compared to the harmonic limit depending on nuclei.

The experimental systematic indicates that the anharmonic effect and the interphonon interaction may play a role in the deviation of the DGDR from its harmonic description. Since the anharmonicity comes from the microscopic mechanism of the excitations and their mutual coupling, the anharmonic effect must be studied based on a microscopic framework. Several microscopic studies have been undertaken in this direction and important results have been obtained.

In a microscopic model explicitly treating $2p2h$ excitations, Nishizaki and Wambach performed calculations for ^{40}Ca and ^{208}Pb [7,8]. Their results for ^{208}Pb [8] show only a small anharmonicity. The DGDR energy is smaller than twice the GDR energy by only few hundred keV for both 0^+ and 2^+ components of the DGDR. The Landau damping is larger than that of the GDR by a factor of 1.12 – 1.17. The spreading and escape widths are not treated in this approach. Similar conclusions have been drawn for ^{40}Ca [7]. For ^{208}Pb the excitation cross section of the GDR and DGDR have been estimated for three choices of the minimum impact parameter. The authors found that none of these choices can explain the measured cross sections simultaneously and hence the discrepancy between measured cross sections and theoretical estimates remains.

Using the quasiparticle-phonon model (QPM) by Soloviev [9], Ponomarev *et al.* [10] took into account the mixing between multiphonon configurations. Despite the complexity of mixing a huge number of configurations up to three-

*On leave of absence from the Institute of Nuclear Science and Technique, VAEC, Hanoi, Vietnam. Electronic address: dang@rikaxp.riken.go.jp

 ©1999 The American Physical Society

phonon states, the numerical results are found to be very close to the predictions by the harmonic picture. The strength distributions of 0^+ and 2^+ components of the DGDR look almost identical.

Going beyond the random-phase approximation (RPA), Lanza *et al.* [11] studied the anharmonicity in the DGDR by mixing two-phonon states among themselves and with one-phonon states. They used a boson mapping technique to introduce nonlinear terms in the external field. These nonlinear terms give the possibility for a direct connection between the ground state and two-phonon states. Due to the constructive interplay of both anharmonicity in configuration mixing and nonlinearity in the external field, the results of their calculations for Coulomb excitation show an enhancement in the cross section in the DGDR region by 10% for ^{208}Pb and 20% for ^{40}Ca. Summing up all the contributions coming from the various states in the vicinity of the DGDR and above the isovector giant quadrupole resonance (IVGQR) ($E>22$ MeV), their calculated cross section for the Pb+Pb reaction at a high incident energy 641 MeV/nucleon became 310 mb, which is fairly close to the experimental value of 380 ± 40 mb. In recent calculations [12], which included both Coulomb and nuclear excitations of the external field, a 25% enhancement of the cross section of the DGDR has been reported for the ^{208}Pb+^{208}Pb collision at an intermediate energy of 50 MeV/nucleon.

An alternative approach to the theoretical study of the DGDR has been proposed by Kurasawa and Suzuki [13] via studying the sum rules of the DGDR excited by a two-step dipole process. By setting the DGDR energy to be exactly twice as large compared to the GDR energy (i.e., the harmonic limit for the DGDR energy), the authors derived a constraint for the sum rule of the DGDR, according to which the non-energy weighted sum of strengths (non-EWSS) $m_0^{(2)}$ of the DGDR is related to $m_0^{(1)}$ for the GDR by $m_0^{(2)}=2[m_0^{(1)}]^2$. They also showed that the width of the DGDR is $\sqrt{2}$ times that of the GDR. However, taking account of the full Hamiltonian including the terms, which contain the sum of products of two pp (hh) pairs (the scattering term), Dinh Dang *et al.* [14] have shown in a schematic model that there is a possibility of the enhancement of the sum of strength of the DGDR as compared to the harmonic limit, because the anharmonic effects due to the scattering term on the EWSS, being small for the GDR, are found enhanced for the DGDR.

Finally, it has been proposed in Ref. [1] that another way to compute the anharmonicity is to consider a DGDR built on a hot rather than a ground-state GDR. Since experiment [15–17] and theory [18–21] have shown that the thermal effect indeed leads to a sharp increase of the GDR width at low temperatures ($T\leqslant3$ MeV) and a saturation of this width at high temperatures ($T>3$ MeV), this behavior should certainly affect the DGDR. However, numerical estimation of the thermal effect on the DGDR is still absent so far.

A general conclusion from these results can be drawn that the anharmonic effects, being small in average parameters of the DGDR such as the width and the energy, may result in a noticeable change in other characteristics such as the excitation cross section. Except for the harmonic picture where the width and energy of the multiphonon resonance can be derived analytically, all the results for these parameters of the DGDR have been provided so far through rather heavy and elaborate calculations. Meanwhile, in order to have further insight into the mechanism of the DGDR, in our opinion, a simple theoretical approach based on the well-established knowledge of the GDR might be useful. The proposal of such an approach is the main goal of the present paper. For this purpose we will make use of the phonon damping model (PDM), which has been proposed recently and applied quite successfully to describe the behavior of the hot GDR in Refs. [18–21]. The method of double-time Green's functions employed in this approach will allow one to make a natural extension to the nonzero temperature.

The present paper is organized as follows. In Sec. II the formalism of the approach is derived. Section III is devoted to the analysis and discussion of numerical results. The paper is summarized in Sec. IV, where conclusions are provided.

II. FORMALISM

A. General

The PDM has been proposed and discussed in detail in Refs. [18–21]. Extending the PDM to the study of the DGDR in the present paper, we hope to be able to explore the possible limit of the applicability and the capability of a model, which has been demonstrated to be effective in describing the behavior of the GDR in hot nuclei.

We use the Hamiltonian of the PDM for the description of the coupling of collective oscillations (phonons) to the field of incoherent nucleon pairs [18–21]. This Hamiltonian is composed of three terms:

$$H=\sum_s E_s a_s^\dagger a_s+\sum_q \omega_q Q_q^\dagger Q_q+\sum_{s,s',q} F_{ss'}^{(q)} a_s^\dagger a_{s'}(Q_q^\dagger+Q_q). \tag{2.1}$$

The first term on the right-hand side (rhs) of Eq. (2.1) is the field of independent single particles, where $a_s^\dagger$ and a_s are creation and destruction operators of a particle or hole state with energy $E_s=\epsilon_s-\epsilon_F$. The energy ϵ_s is the single-particle energy and ϵ_F the Fermi energy. We will call the energy E_s the single-particle energy whenever there is no confusion with ϵ_s. The second term stands for the phonon field as the field of harmonic oscillators, where $Q_q^\dagger$ and Q_q are the creation and destruction operators of a phonon with energy ω_q. The last term describes the coupling between the first two terms. The indices s and s' denote particle (p, $E_p>0$) or hole (h, $E_h<0$), while the index q is reserved for the phonon state $q=\{\lambda,i\}$ with multipolarity λ (the projection μ of λ in the phonon index is omitted for simplicity). Hence, the last term on the rhs of Eq. (2.1) includes the coupling between the phonon field and all possible ph, pp, and hh pairs. In general, the sums in the last two terms on the rhs of Eq. (2.1) are carried out over $\lambda\geqslant1$. This form of the model Hamiltonian in Eq. (2.1) is quite general and common in many microscopic approaches to nuclear collective excitations. The difference is in the way of defining the single-particle energy E_s, phonon energy ω_q, and phonon structure under a specific effective coupling $F_{ss'}^{(q)}$. In the QPM [9] or the nuclear field theory (NFT) [22], e.g., the coupling vertex $F_{ss'}^{(q)}$ is a sum of products of the coupling strength and the coupling-matrix elements. The coupling strength contains the

RPA amplitudes of ph configurations in the collective oscillation. The coupling matrix elements can be obtained through the derivative of the central potential. In the QPM, the phonon operators $Q_q^\dagger$ and Q_q have the fermion structure, being built from the coherent ph or quasiparticle pairs. The form in Eq. (2.1) has been derived rigorously from the QPM Hamiltonian in Ref. [23]. In the simplest case when the two-body term consists of only a separable isovector dipole-dipole interaction, one recovers from Eq. (2.1) the Hamiltonian, widely used in the literature to describe the g.s. GDR [24].

We consider the damping of the two-phonon excitation as the result of coupling of two single-phonon excitations, each of which is undergoing the damping due to coupling to incoherent nucleon pairs. In order to study this process, we introduce the following double-time Green's functions which describe:

(1) The propagation of two free phonons:

$$G_{q_1q_2;q_1'q_2'}(t-t')=\langle\langle Q_{q_1}(t)Q_{q_2}(t);Q_{q_1'}^\dagger(t')Q_{q_2'}^\dagger(t')\rangle\rangle. \tag{2.2}$$

(2) The transition between ''nucleon pair $\otimes$ phonon'' and two-phonon configurations:

$$\mathcal{G}_{ss'q;q_1'q_2'}(t-t')=\langle\langle a_s^\dagger(t)a_{s'}(t)Q_q(t);Q_{q_1'}^\dagger(t')Q_{q_2'}^\dagger(t')\rangle\rangle. \tag{2.3}$$

In Eqs. (2.2) and (2.3) the standard notation for the retarded double-time Green's function is used [25,26], which means

$$\langle\langle A(t);B(t')\rangle\rangle=-i\theta(t-t')\{\langle A(t)B(t')\rangle\mp\langle B(t')A(t)\rangle\}, \tag{2.4}$$

for any operators $A(t)$ and $B(t')$ with $\langle\ldots\rangle$ denoting the average over the grand canonical ensemble at temperature T. According to the standard method [26], the equation of motion for the double-time Green's function $\langle\langle A(t);B(t')\rangle\rangle$ with respect to the Hamiltonian H can be derived from

$$i\frac{d}{dt}\langle\langle A(t);B(t')\rangle\rangle=\delta(t-t')\langle[A(t),B(t)]\rangle+\langle\langle[A(t),H(t)];B(t')\rangle\rangle. \tag{2.5}$$

The double-time Green's functions are convenient for applications in statistics as they can be analytically continued in the complex plane. This allows one to derive the damping of the resonance as the imaginary part of the polarization operator in a straightforward manner, avoiding the ambiguity in estimating the resonance width via the variation of the second moment [21]. In Ref. [20] we have shown that the PDM contains a large class of graphs, including those of the nuclear field theory (NFT) [22].

Applying Eq. (2.5) to function (2.2) and Hamiltonian (2.1), we obtain the following exact equation, which couples function (2.2) to function (2.3):

$$\begin{aligned}i\frac{d}{dt}G_{q_1q_2;q_1'q_2'}(t-t')&=\delta(t-t')(1+\nu_{q_1}+\nu_{q_2})(\delta_{q_1q_1'}\delta_{q_2q_2'}+\delta_{q_1q_2'}\delta_{q_1'q_2})\\&+(\omega_{q_1}+\omega_{q_2})G_{q_1q_2;q_1'q_2'}(t-t')\\&+\sum_{s,s'}[F_{ss'}^{(q_1)}\mathcal{G}_{ss'q_2;q_1'q_2'}(t-t')\\&+F_{ss'}^{(q_2)}\mathcal{G}_{ss'q_1;q_1'q_2'}(t-t')].\end{aligned} \tag{2.6}$$

In Eq. (2.6) the phonon occupation number ν_q at the phonon energy ω_q occurs as a result of averaging over the grand canonical ensemble

$$\langle Q_q^\dagger Q_{q'}\rangle=\delta_{qq'}\nu_q. \tag{2.7}$$

The equation for the function (2.3), that enters in the rhs of Eq. (2.6), is derived from Eq. (2.5) in the same way. The exact result contains the function (2.3), as well as the higher-order Green's functions in the rhs. These higher-order Green functions are

(a) $\langle\langle a_s^\dagger(t)a_{s''}(t)Q_{q'}(t)Q_q(t);Q_{q_1'}^\dagger(t')Q_{q_2'}^\dagger(t')\rangle\rangle$,
(b) $\langle\langle a_s^\dagger(t)a_{s''}(t)Q_{q'}^\dagger(t)Q_q(t);Q_{q_1'}^\dagger(t')Q_{q_2'}^\dagger(t')\rangle\rangle$,
(c) $\langle\langle a_s^\dagger(t)a_{s'}(t)a_{s_1}^\dagger(t');Q_{q_1'}^\dagger(t')Q_{q_2'}^\dagger(t')\rangle\rangle$.

The hierarchy of the Green's function would continue unless a decoupling is introduced to obtain a closed set of equations. The degree of complexity in the configuration mixing depends, therefore, on the way of truncating the chain of equations. Since several numerical calculations (see, e.g., Ref. [10]) have shown that higher-order effects such as coupling to three-phonon configurations, etc. seem to be negligible on the damping of the two-phonon resonance, we will confine ourselves in this work to the lowest-order coupling, considering only functions (2.2) and (2.3). Therefore, we apply the decoupling scheme in Ref. [26] to approximate the Green's function (a) as

$$\langle\langle a_s^\dagger(t)a_{s''}(t)Q_{q'}(t)Q_q(t);Q_{q_1'}^\dagger(t')Q_{q_2'}^\dagger(t')\rangle\rangle\approx\delta_{ss''}n_sG_{q'q;q_1'q_2'}(t-t'), \tag{2.8}$$

where n_s is the single-particle occupation number

$$n_s=\langle a_s^\dagger a_s\rangle. \tag{2.9}$$

The contribution of the Green's function (b) can be neglected because it is associated with the so-called scattering-phonon process, which may become important only in the phonon excitation at very low energy. Applying the same decoupling to the function (c), we find that the remaining Green's function is of the type $\langle\langle a_s^\dagger(t)a_{s''}(t);Q_{q_1'}^\dagger(t')Q_{q_2'}^\dagger(t')\rangle\rangle$. In Ref. [19] it has been shown that this type of Green's function is related to the single-particle damping, whose contribution to the damping of the collective phonon excitation such as the GDR can be omitted in the first order. This allows us to

neglect also the contribution of function (c) in all further considerations in the present paper.

Within this approximation scheme the equation for function (2.3) can be truncated to the following form:

$$i\frac{d}{dt}\mathcal{G}_{ss'q;q_1'q_2'}(t-t')=(E_{s'}-E_s+\omega_q)\mathcal{G}_{ss'q;q_1'q_2'}(t-t') + \sum_{q'} F_{s's}^{(q')}(n_s-n_{s'})G_{q'q;q_1'q_2'}(t-t'). \tag{2.10}$$

Making now the Fourier transform of Eqs. (2.6) and (2.10) to the energy plane E, we obtain the following set of equations:

$$(E-\omega_{q_1}-\omega_{q_2})G_{q_1q_2;q_1'q_2'}(E) - \sum_{s_1,s_1'} F_{s_1s_1'}^{(q_1)}\mathcal{G}_{s_1s_1'q_2;q_1'q_2'}(E) - \sum_{s_1,s_1'} F_{s_1s_1'}^{(q_2)}\mathcal{G}_{s_1s_1'q_1;q_1'q_2'}(E) = \frac{1}{2\pi}(1+\nu_{q_1}+\nu_{q_2})(\delta_{q_1q_1'}\delta_{q_2q_2'}+\delta_{q_1q_2'}\delta_{q_1'q_2}), \tag{2.11}$$

$$(E-E_{s'}+E_s-\omega_q)\mathcal{G}_{ss'q;q_1'q_2'}(E) - \sum_{q'} F_{s's}^{(q')}(n_s-n_{s'})G_{q'q;q_1'q_2'}(E)=0. \tag{2.12}$$

Expressing $\mathcal{G}_{ss'q;q_1'q_2'}(E)$ in terms of $G_{q'q;q_1'q_2'}(E)$ using Eq. (2.12) and inserting the result in Eq. (2.11), we obtain an equation for $G_{q'q;q_1'q_2'}(E)$. For the propagation of a two-phonon configuration $(q_1,q_2)=(q_1',q_2')$ this equation takes a simple form as

$$G_{q_1q_2}(E)=\frac{1}{\pi}\frac{1+\nu_{q_1}+\nu_{q_2}}{E-\omega_{q_1}-\omega_{q_2}-P_{q_1q_2}(E)}, \tag{2.13}$$

where the two-phonon polarization operator $P_{q_1q_2}(E)$ has the form

$$P_{q_1q_2}(E)=\sum_{s,s'}(n_s-n_{s'})\left[\frac{F_{ss'}^{(q_1)}F_{s's}^{(q_1)}}{E-E_{s'}+E_s-\omega_{q_2}} + \frac{F_{ss'}^{(q_2)}F_{s's}^{(q_2)}}{E-E_{s'}+E_s-\omega_{q_1}}\right]. \tag{2.14}$$

In Eqs. (2.11) and (2.14) we omit the indices (q_1',q_2') as they coincide with (q_1,q_2).

The damping and the energy shift of two-phonon excitation are calculated as the imaginary part and real part of the analytic continuation of polarization operator $P_{q_1q_2}(E)$ into the complex energy plane $E=\omega\pm i\varepsilon$ (ω is real and $\varepsilon\to 0$), respectively [18–21,26]. The analytical form of the damping is obtained in this way as

$$\gamma_{q_1q_2}(\omega)=\pi\left|\sum_{s,s'}(n_s-n_{s'})[F_{ss'}^{(q_1)}F_{s's}^{(q_1)}\delta(\omega-E_{s'}+E_s-\omega_{q_2}) + F_{ss'}^{(q_2)}F_{s's}^{(q_2)}\delta(\omega-E_{s'}+E_s-\omega_{q_1})]\right|, \tag{2.15}$$

while the energy shift has the form

$$P_{q_1q_2}(\omega)=\mathcal{P}\sum_{s,s'}(n_s-n_{s'})\left[\frac{F_{ss'}^{(q_1)}F_{s's}^{(q_1)}}{\omega-E_{s'}+E_s-\omega_{q_2}} + \frac{F_{ss'}^{(q_2)}F_{s's}^{(q_2)}}{\omega-E_{s'}+E_s-\omega_{q_1}}\right], \tag{2.16}$$

with $\mathcal{P}$ denoting the principal value of the corresponding integral. The excitation energy of the two-phonon state is defined as the solution $\bar{\omega}$ of the equation for the pole of the Green's function (2.11), that is

$$\bar{\omega}-(\omega_{q_1}+\omega_{q_2})-P_{q_1q_2}(\bar{\omega})=0. \tag{2.17}$$

Equations (2.15)–(2.17) are the main equations for the study of two-phonon excitations within the present formalism. If the damping of each single-phonon excitation is described by a microscopic model such as the PDM [18–21], the phonon occupation number ν_q (single-particle occupation number n_s) used in the calculations of the DGDR can be approximated by the Bose-Einstein (Fermi-Dirac) distribution at the phonon energy ω_q (single-particle energy E_s) and temperature T [19]. We also notice that the presence of the factor $(n_s-n_{s'})$ on the rhs of Eqs. (2.15) and (2.16) implies that at $T=0$ only the coupling to ph configurations contributes to the damping of the two-phonon excitation since $n_h=1$ and $n_p=0$, while at $T\neq 0$ the coupling to pp and hh configurations will become dominant with increasing T. The latter leads to the sharp increase of the GDR width at low T and its saturation at high T. Detailed discussions on this issue are given in Refs. [19–21]. Thus, this formalism allows a natural extension to the nonzero temperature case.

We notice that the decoupling scheme in Eq. (2.8) partially includes the Pauli-correction terms in a sense of average. These terms consist of the matrix elements $\langle 0|Q_{q_1'}Q_{q_2'}HQ_{q_1}^{\dagger}Q_{q_2}^{\dagger}|0\rangle$ [1], which become in the present approach

$$\langle 0|Q_{q_1'}Q_{q_2'}HQ_{q_1}^{\dagger}Q_{q_2}^{\dagger}|0\rangle = \sum_{q,s,s'} F_{ss'}^{(q)}\langle 0|Q_{q_1'}Q_{q_2'}a_s^{\dagger}a_{s'}(Q_q^{\dagger}+Q_q)Q_{q_1}^{\dagger}Q_{q_2}^{\dagger}|0\rangle, \tag{2.18}$$

where $|0\rangle$ is the phonon vacuum at $T=0$. Expanding the nucleon pair $a_s^{\dagger}a_{s'}$ in the boson space into series of boson operators according to the mapping in Ref. [27], we can see that the expansion of $a_p^{\dagger}a_{p'}$ ($a_h^{\dagger}a_{h'}$) into a sum of tensor products of two ph bosons yields a zero value of the matrix element (2.18) because of the odd number of boson operators within the average. The mapping of $a_h^{\dagger}a_p$ into the series of

boson operators leads to three-boson terms in the two-phonon space for the matrix element (2.18) except for the lowest-order term. The latter is taken into account by the function (2.3) within the decoupling (2.8). In general, it is known that the Pauli-correction terms may cause a shift of relative order $\sim A^{-2/3}$ from the harmonic estimate of the two-phonon energy [28], which amounts to only ~ 0.03–0.05 MeV for $90 \leqslant A \leqslant 208$. The recent study by Bertsch and Feldmeier in Ref. [29] using the variational approach to anharmonic collective motion has found an even smaller shift of order $\sim A^{-4/3}$ of the second phonon energy for all three modes: monopole, dipole, and quadrupole.

B. Double giant dipole resonance

The DGDR can be considered as a special case of the general formalism in the previous Sec. II A, namely when the two single-phonon excitations coincide $q_1 = q_2 = q$. Their unperturbed energies are denoted, in this case, as

$$\omega_{q_1} = \omega_{q_2} = \omega_q , \tag{2.19}$$

where the index q denotes the collective one-phonon state with multipolarity and parity $\lambda^\pi = 1^-$ and energy ω_q (the unperturbed giant dipole oscillation). From Eqs. (2.13)–(2.17) we easily obtain the equations for the DGDR. Namely, for the propagation of DGDR we have

$$G_{qq}(E) = \frac{1}{\pi} \frac{1 + 2\nu_q}{E - 2\omega_q - P_{qq}(E)} \tag{2.20}$$

with the polarization operator

$$P_{qq}(E) = 2 \sum_{s,s'} (n_s - n_{s'}) \frac{F^{(q)}_{ss'} F^{(q)}_{s's}}{E - E_{s'} + E_s - \omega_q}. \tag{2.21}$$

The damping and the energy shift of the DGDR are, respectively,

$$\gamma_{qq}(\omega) = 2\pi \left| \sum_{s,s'} (n_s - n_{s'}) F^{(q)}_{ss'} F^{(q)}_{s's} \delta(\omega - E_{s'} + E_s - \omega_q) \right|, \tag{2.22}$$

$$P_{qq}(\omega) = 2\mathcal{P} \sum_{s,s'} (n_s - n_{s'}) \frac{F^{(q)}_{ss'} F^{(q)}_{s's}}{\omega - E_{s'} + E_s - \omega_q}. \tag{2.23}$$

The full width at the half maximum (FWHM) of the DGDR is defined as twice the damping in Eq. (2.22) at the DGDR energy ω_{DGDR}, namely

$$\Gamma_{\mathrm{DGDR}} = 2\gamma_{qq}(\omega_{\mathrm{DGDR}}). \tag{2.24}$$

The energy ω_{DGDR} of the DGDR is the solution of the equation

$$\omega_{\mathrm{DGDR}} - 2\omega_q - P_{qq}(\omega_{\mathrm{DGDR}}) = 0. \tag{2.25}$$

If we now recall that the energy ω_{GDR} of the GDR is defined in the simplest version, the PDM-1 [18,19] by the equation

$$\omega_{\mathrm{GDR}} - \omega_q - P_q(\omega_{\mathrm{GDR}}) = 0 \tag{2.26}$$

with

$$P_q(\omega) = \mathcal{P} \sum_{s,s'} (n_s - n_{s'}) \frac{F^{(q)}_{ss'} F^{(q)}_{s's}}{\omega - E_{s'} + E_s}, \tag{2.27}$$

we can derive the shift of the DGDR energy ω_{DGDR} from its harmonic value $2\omega_{\mathrm{GDR}}$ making use of Eqs. (2.25) and (2.26) as

$$\omega_{\mathrm{DGDR}} - 2\omega_{\mathrm{GDR}} = P_{qq}(\omega_{\mathrm{DGDR}}) - 2P_q(\omega_{\mathrm{GDR}}). \tag{2.28}$$

Using Eqs. (2.22) and (2.24) for the DGDR width and the expression for the GDR width from Refs. [18,19], we obtain the ratio

$$\frac{\Gamma_{\mathrm{DGDR}}}{\Gamma_{\mathrm{GDR}}} = 2 \frac{\sum_{ss'} (n_s - n_{s'}) F^{(q)}_{ss'} F^{(q)}_{s's} \delta(\omega_{\mathrm{DGDR}} - \omega_q - E_{s'} + E_s)}{\sum_{ss'} (n_s - n_{s'}) F^{(q)}_{ss'} F^{(q)}_{s's} \delta(\omega_{\mathrm{GDR}} - E_{s'} + E_s)}. \tag{2.29}$$

It can be seen from Eq. (2.29) that in the harmonic limit, when $|P_{qq}(\omega_{\mathrm{DGDR}})| \ll \omega_{\mathrm{DGDR}}$ and $|P_q(\omega_{\mathrm{GDR}})| \ll \omega_{\mathrm{GDR}}$ so that $\omega_{\mathrm{DGDR}} \simeq 2\omega_q$ and $\omega_{\mathrm{GDR}} \simeq \omega_q$, the ratio (2.29) becomes just 2 and the shift in Eq. (2.28) vanishes. In general, employing the δ-function representation $\delta(x) = \varepsilon[\pi(x^2 + \varepsilon^2)]^{-1}$, we see that many components under the sums on the rhs of Eq. (2.29) satisfy the inequality

$$\frac{1}{[\omega_{\mathrm{DGDR}} - \omega_q - (E_{s'} - E_s)]^2} < \frac{1}{[\omega_{\mathrm{GDR}} - (E_{s'} - E_s)]^2}, \tag{2.30}$$

since an inequality $\omega_q > E_{s'} - E_s$ always holds for the case with $(s,s') = (p,h)$ and ω_q located close to the energy of the GDR. Thus, we have

$$\Gamma_{\mathrm{DGDR}} < 2\Gamma_{\mathrm{GDR}}, \tag{2.31}$$

which has been actually observed in the experiments.

Similarly to the strength function $S_q(\omega)$ of the GDR derived in Ref. [20], the strength function $S_{qq}(\omega)$ of the DGDR is derived from Eq. (2.20) as

$$S_{qq}(\omega) = \frac{1}{\pi} \frac{\gamma_{qq}(\omega)(1 + 2\nu_{\mathrm{GDR}})}{(\omega - \omega_{\mathrm{DGDR}})^2 + [\gamma_{qq}(\omega)]^2}, \tag{2.32}$$

where ν_{GDR} denotes the phonon occupation number ν_q defined at energy $\omega_q = \omega_{\mathrm{GDR}}$.

Since two virtual photons are absorbed to excite the DGDR through the Coulomb excitation process, those virtual photons are replaced by the equivalent real photons when we apply the Weizsäcker-Williams method [30]. According to this method, the Coulomb excitation cross section σ_C is related to the equivalent photon number n_{λ^π} and the photoabsorption cross section $\sigma_\gamma^{(\lambda^\pi)}(\omega)$ as

$$\sigma_C = \sum_\lambda \int \frac{n_{\lambda^\pi}}{\omega} \sigma_\gamma^{(\lambda^\pi)}(\omega) d\omega. \tag{2.33}$$

The photoabsorption cross section $\sigma_{\gamma}^{(\lambda^{\pi})}(\omega) \equiv \sigma_{qq}(\omega)$ for the DGDR in Eq. (2.33) can be formally defined from the strength function (2.32) as

$$\sigma_{qq}(\omega) \propto S_{qq}(\omega)\gamma_{qq}(\omega)\frac{\omega}{\omega_{\mathrm{DGDR}}}. \tag{2.34}$$

Therefore, we have some hope to infer the possible change in the electromagnetic cross section from the change in the photoabsorption cross section of the DGDR due to anharmonic effect. While this may reveal the source of the change in the electromagnetic cross section, there still remains a question on how to measure this photoabsorption cross section for the DGDR.

The EWSS and non-EWSS are calculated from the kth moment

$$m_k^{(i)} = \int_{E_1}^{E_2} S_j(\omega)\omega^k d\omega, \tag{2.35}$$

where the notation $(i=1,\ j=q)$ corresponds to the GDR case, while $(i=2,\ j=qq)$ is reserved for the DGDR. The calculated values of the moments should be compared with the sum-rule constraints discussed in Ref. [13].

III. NUMERICAL RESULTS

In this section we present the results of the calculations of various DGDR characteristics such as energy, FWHM, strength function, photoabsorption cross section, EWSS and non-EWSS, whose expressions have been derived in Sec. II B. The calculations are performed for three nuclei ^{90}Zr, ^{120}Sn, and ^{208}Pb at zero and nonzero temperatures. In order to determine the GDR, we employ the same scenario, which has been successfully used in the description of the hot GDR within the PDM-1 [18,19]. The latter is much simpler than the PDM-2 where the coupling to more complicated configurations is explicitly included [20,21]. In this scenario, we assume that a fully microscopic description of the structure of the ground-state GDR and its spreading width $\Gamma^{\downarrow}$ would not be important in the present consideration. In fact such a description can be found in a number of works such as Refs. [9,22]. Various microscopic calculations and experimental data have shown that the GDR can be considered as a strongly collective one-phonon excitation. Therefore, in order to have a simple and clear picture, we assume that the ground-state GDR is generated by a single collective and structureless phonon with energy ω_q close to the centroid energy ω_{GDR} of the ground-state GDR. We employ realistic single-particle energies, calculated in the Woods-Saxon potentials at $T=0$ for the nuclei under consideration. In the PDM-1 reasonable agreement between theory and data has been achieved via coupling of GDR phonon to all ph, pp, and hh configurations. The phonon energy ω_q and the matrix elements of the coupling to ph and pp or hh $F_{ph}^{(q)} = F_1$ for $(s,s') = (p,h)$, and $F_{pp}^{(q)} = F_{hh}^{(q)} = F_2$ for $(s,s') = (p,p')$ or (h,h') are introduced as parameters. Even though the higher-order graphs were not included explicitly in the equations within the PDM-1, this procedure implies that they are incorporated effectively in the parameters F_1 and F_2. The energy ω_q and the parameters F_1 and F_2 for the couplings have been chosen so that the experimental width and energy of the GDR at $T=0$ are reproduced, and that the GDR energy does not vary with changing T (see the details in Ref. [19]). Since these values are independent of temperature, all the thermal effects exclusively come from the microscopic configuration mixing. The parameters employed in the present calculations of the DGDR are the same as those defined within the PDM-1 and presented in Table I of Ref. [19]. The calculations have also used a value of 0.5 MeV for the smearing parameter ε in the δ function. It has been confirmed that the results are stable against the variation of ε within the interval 0.2 MeV$\leqslant\varepsilon\leqslant$1.0 MeV.

TABLE I. Widths and energies (in MeV) of the GDR and DGDR. The subscript 1 denotes the GDR, while 2 stands for DGDR.

	Γ_2	E_2	Γ_1	E_1	$2\Gamma_1$	$\sqrt{2}\Gamma_1$	$2E_1$
^{90}Zr	6.49	32.2	4.2	16.3	8.4	5.94	32.9
^{120}Sn	6.05	30.8	4.8	15.4	9.6	6.79	30.8
^{208}Pb	7.95	27.6	4.0	13.7	8.0	5.66	27.4

A. Results at zero temperature

The calculated widths and energies of the DGDR in ^{90}Zr, ^{120}Sn, and ^{208}Pb are compared with the corresponding values of the GDR and those in the harmonic picture in Tables I and II. In Table II the experimental ratios for the widths and energies of DGDR and GDR are also shown.

The energy of the DGDR $\omega_{\mathrm{DGDR}} \equiv E_2$ is found to be shifted down by 0.7 MeV in ^{90}Zr and up by 0.2 MeV in ^{208}Pb as compared to their harmonic values of $2\omega_{\mathrm{GDR}} \equiv 2E_1$. In the case of ^{120}Sn the DGDR energy is found to be just twice as large compared to the GDR energy. The widths Γ_{DGDR} (Γ_2 in the tables) of the DGDR in ^{90}Zr and ^{208}Pb are found to be in between $\sqrt{2}\Gamma_{\mathrm{GDR}}$ and $2\Gamma_{\mathrm{GDR}}$ ($\Gamma_{\mathrm{GDR}} = \Gamma_1$ in the tables). In ^{120}Sn the DGDR width Γ_{DGDR} is even smaller than $\sqrt{2}\Gamma_{\mathrm{GDR}}$. These values agree well with the experimental ones within the error bars (Table II). In general, the

TABLE II. Ratios of widths and of energies of the GDR and DGDR. The notation is the same as in Table I.

	$\Gamma_2/(2\Gamma_1)$	$\Gamma_2/(\sqrt{2}\Gamma_1)$	Γ_2/Γ_1	$\Gamma_2/\Gamma_1^{(\mathrm{exp})}$	$E_2/(2E_1)$	E_2/E_1	$E_2/E_1^{(\mathrm{exp})}$
^{90}Zr	0.77	1.09	1.55	1.7±0.25 [1]	0.98	1.98	1.9±0.5 [1]
^{120}Sn	0.63	0.89	1.26	1.7±0.7 [1]	1.00	2.00	2.05±0.5 [1]
^{208}Pb	0.99	1.40	1.99	3.0±1.25 [4]	1.01	2.02	1.87±0.1 [4]

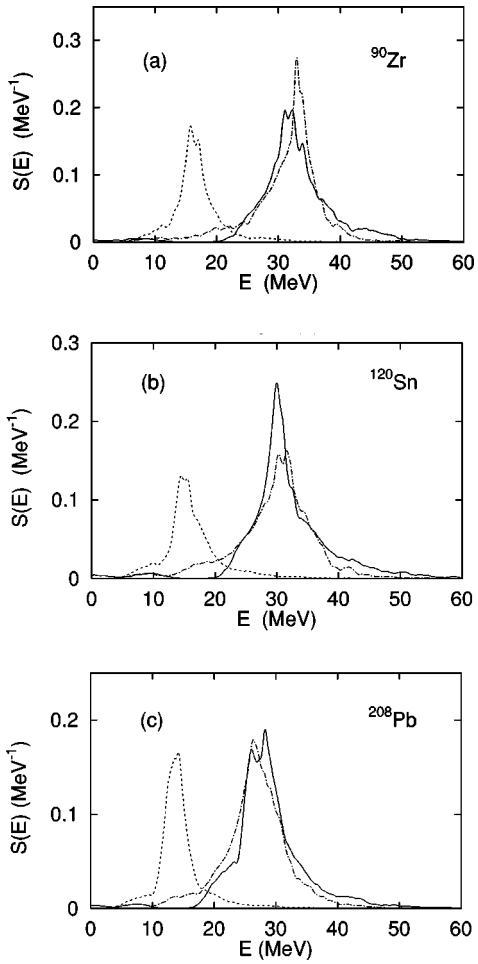

FIG. 1. Strength functions of the GDR and DGDR. In each panel the dashed curve is the strength function of the GDR. The solid curve represents the strength function of the DGDR. The dash-dotted curve corresponds to the harmonic limit of the strength function of the DGDR.

DGDR energy is quite well reproduced by the independent phonon picture in all three nuclei. Regarding the width, one can see that the DGDR in ^{208}Pb seems to behave like a quite good superposition of two noninteracting GDRs, while the deviation from the harmonic limit for the width of the DGDR in ^{90}Zr and ^{120}Sn is more noticeable. The difference between the behavior of the DGDR in double-magic nuclei and the one in open-shell nuclei has been also pointed out recently in the microscopic calculations by Lanza *et al.* [11]. We notice that since the DGDR is composed of a GDR built on another GDR, the degree of collectivity of the GDR, which shows how close the vibration is to the harmonic oscillation, will certainly imply the degree of harmonicity in the DGDR. As a matter of fact the GDR in ^{208}Pb is very collective with a rather small width $\Gamma_{\mathrm{GDR}} \simeq 4$ MeV. Consequently, the anharmonicity in the DGDR in ^{208}Pb is minimal as can be expected. The anharmonic effect on the GDR in ^{120}Sn is the strongest among three nuclei giving the largest width $\Gamma_{\mathrm{GDR}} \simeq 4.8$ MeV of the GDR. Therefore the DGDR width $\Gamma_{\mathrm{DGDR}} = 6.05$ MeV in this nucleus also deviates strongly from its harmonic value of $2\Gamma_{\mathrm{GDR}} = 9.6$ MeV.

The calculated strength functions of the GDR and DGDR are shown in Fig. 1. The harmonic limit of the DGDR shape is obtained by replacing ω_{DGDR} and $\gamma_{qq}(\omega)$ in Eq. (2.32) with two times of the corresponding values for the GDR, i.e., with $2\omega_{\mathrm{GDR}}$ and $2\gamma_q(\omega)$, respectively. A noticeable difference between the shape of the DGDR and its harmonic limit is seen in ^{90}Zr and ^{120}Sn, in particular in ^{120}Sn. For the DGDR in ^{208}Pb the difference is much less. It is important to notice that neither the GDR strength function $S_q(\omega)$ [20,21] nor the DGDR strength function $S_{qq}(\omega)$ in Eq. (2.32) is given as a single Breit-Wigner curve. In fact they are composed of many Breit-Wigner shapes because of the ω-dependent damping $\gamma_q(\omega)$ in the GDR or $\gamma_{qq}(\omega)$ in DGDR. Therefore, the DGDR energy ω_{GDR} defined as the solution of Eq. (2.25) can be assigned to the DGDR centroid energy, but not to its maximum peak. Only in the case when the strength function can be well approximated by a single Breit-Wigner curve as in the GDR, the energy centroid may coincide with the position of the maximum peak of the resonance. This explains why the shift between the maximum peaks of the solid and dash-dotted lines in Fig. 1 is slightly larger than the difference between the (centroid) energy of the GDR and its corresponding value in the harmonic limit shown in Table II.

In Ref. [13], Kurasawa and Suzuki have derived the relation

$$s_1 \equiv \frac{m_1^{(2)}}{4m_0^{(1)}m_1^{(1)}} = 1, \tag{3.1}$$

and by putting $\omega_{\mathrm{DGDR}} = 2\omega_{\mathrm{GDR}}$, they obtained

$$s_0 \equiv \frac{m_0^{(2)}}{2[m_0^{(1)}]^2} = 1 \tag{3.2}$$

as a sum-rule constraint on the strength of the DGDR. In order to see how these relations are fulfilled, we collect in Table III the values of the corresponding moments obtained after integrating over $0 \leqslant \omega \leqslant 60$ MeV. The results in Table III show that the closest values to the relation (3.1) can be

TABLE III. Values of zero (non-EWSS) and first (EWSS) moments of the GDR and DGDR within $0 \leqslant \omega \leqslant 60$ MeV. The superscript (1) corresponds to GDR, (2) to DGDR. The notation (har) indicates the value calculated in the harmonic limit.

	$m_0^{(1)}$	$m_1^{(1)}$	$m_0^{(2)}$	$m_1^{(2)}$	$m_0^{(2)}$(har)	$m_1^{(2)}$(har)	$4m_0^{(1)}m_1^{(1)}$	$2[m_0^{(1)}]^2$
^{90}Zr	0.94	15.81	1.76	57.41	1.73	53.64	59.45	1.76
^{120}Sn	0.83	13.66	1.84	57.93	1.63	48.24	45.51	1.39
^{208}Pb	0.84	12.26	1.66	47.44	1.62	42.94	41.20	1.41

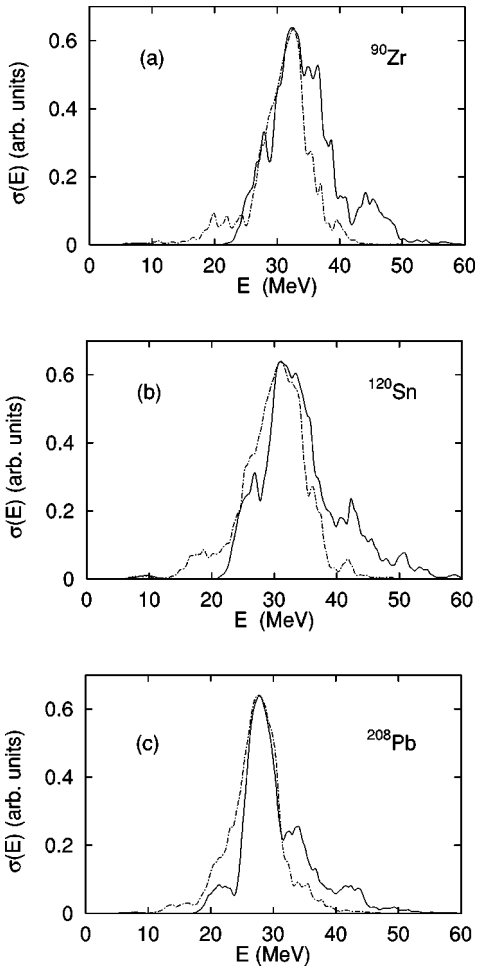

FIG. 2. Photoabsorption cross sections of the DGDR. The notation is the same as in Fig. 1.

obtained only in the harmonic picture, i.e., with $m_1^{(2)}$(har), where we have $s_1=0.9$, 1.06, and 1.04, $s_0=0.98$, 1.17, and 1.15 for ^{90}Zr, ^{120}Sn, and ^{208}Pb, respectively. Otherwise these ratios can reach as much as $s_1=1.27$ and $s_0=1.32$ in ^{120}Sn. Since the non-EWSS $m_0^{(1)}=\langle 0|D^2|0\rangle$ with the dipole operator D entering in Eqs. (3.1) and (3.2) is model-dependent (e.g., it is fulfilled within the Tamm-Dancoff approximation but violated within the RPA), the deviation from relations (3.1) and (3.2) should depend on how anharmonicity is included as has been seen here.

The anharmonic effect on the behavior of the DGDR is best seen in the calculated photoabsorption cross sections shown in Fig. 2. Even though the resonance peak is still at the same place as compared to the harmonic limit (dash-dotted curves), a substantial amount of strength is redistributed toward the high-energy wing. As a result the values of the integrated photoabsorption cross section (IPACS) within the energy interval 22 MeV $\leqslant\omega\leqslant$60 MeV are found to be enhanced by 46%, 22%, and 8% for the DGDR in ^{90}Zr, ^{120}Sn, and ^{208}Pb, respectively (Table IV). These results show that the anharmonic effect, mostly seen in the resonance width as it is due to coupling of phonons to incoherent nucleon pairs, indeed leads to a noticeable enhancement in the photoabsorption cross section of the DGDR as compared to its value in the harmonic picture. Since the photoabsorption cross section is related to the cross section of electromagnetic excitations via Eq. (2.33), the obtained results should contribute ultimately to the enhancement of the cross section in the Coulomb excitation.

TABLE IV. Integrated photoabsorption cross sections σ_2 (in MeV) for the DGDR within 22 MeV$\leqslant\omega\leqslant$60 MeV.

	σ_2	σ_2(har)	σ_2/σ_2(har)	Enhancement
^{90}Zr	7.09	4.87	1.46	46%
^{120}Sn	7.77	6.39	1.22	22%
^{208}Pb	5.23	4.84	1.08	8%

B. Results at nonzero temperature

The strength functions $S_{qq}(\omega)$ from Eq. (2.32) of the DGDR in three nuclei are plotted in Fig. 3 at several temperatures. Since the DGDR damping $\gamma_{qq}(\omega)$ from Eq. (2.22) contains the same factor $n_s-n_{s'}$ as the GDR damping in Refs. [18,19], one expects the same temperature dependence of the DGDR width as compared to the GDR width. This is due to the fact that the value $|n_h-n_p|$, related to the quantal width Γ_Q, always decreases from 1 at $T=0$ with increasing T, while $|n_p-n_{p'}|$ ($|n_p-n_{p'}|$), related to the thermal width Γ_T, increases from 0 at $T=0$ as T increases to some intermediate value, but decreases later on as T increases to very

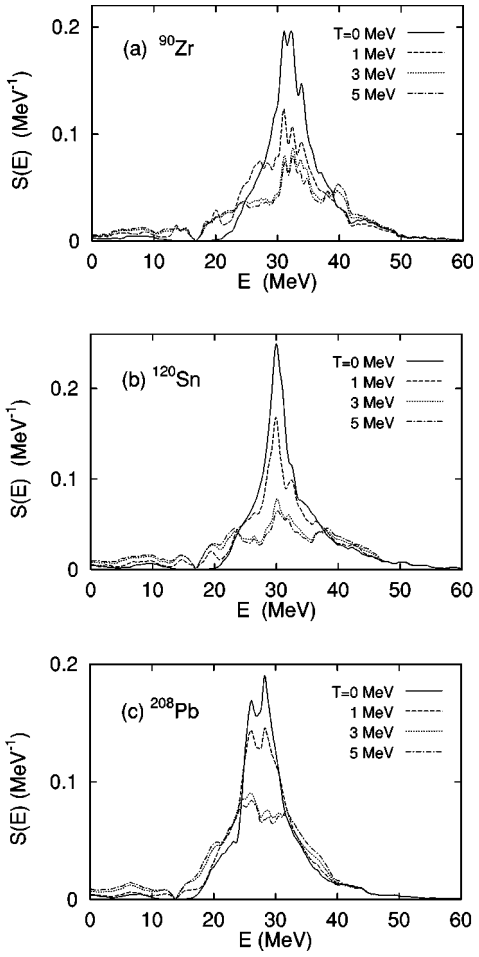

FIG. 3. Strength functions of the DGDR at various temperatures.

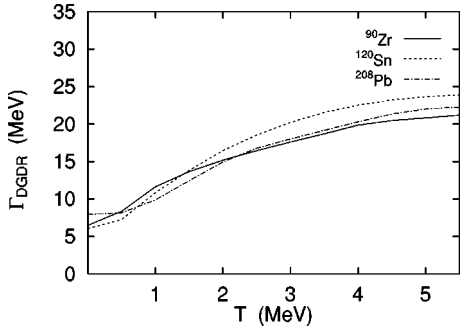

FIG. 4. Width of the DGDR as a function of temperature.

high values. The region where the factors $|n_p - n_{p'}|$ and $|n_h - n_{h'}|$ are around their maximum values corresponds to the region of the width saturation, which has been experimentally observed for the GDR in hot nuclei [16,17]. It can be seen in Fig. 3 that, with the resonance energy located almost at the same place, the width of the DGDR also increases sharply as T increases from 0 up to $T \simeq 3$ MeV. At $T \geqslant 3$ MeV the shape of the DGDR obviously reaches a saturation.

The total width Γ_{GDR} of the DGDR in three nuclei are plotted as a function of temperature in Fig. 4. The saturated values of Γ_{GDR} are around 21, 24, and 22.5 MeV for ^{90}Zr, ^{120}Sn, and ^{208}Pb, respectively. Since the quantal width Γ_Q is due to the anharmonic coupling of the resonance phonons to $1p1h$ configurations, the decrease of the quantal width with increasing T signals the decrease of anharmonicity. Indeed, as shown in Fig. 5, where the ratio $\Gamma_{\mathrm{DGDR}}/\Gamma_{\mathrm{GDR}}$ is plotted as a function of T, the harmonic limit $(\Gamma_{\mathrm{DGDR}}/\Gamma_{\mathrm{GDR}})_{\mathrm{har}} = 2$ seems to be satisfactorily restored at $T \geqslant 1.5$ MeV in ^{90}Zr and ^{120}Sn, while the DGDR width in ^{208}Pb remains always equal to $2\Gamma_{\mathrm{GDR}}$ at all temperatures. The restoration of harmonicity in the DGDR at $T \neq 0$ found in the present study is of paramount importance. The pure harmonic double-phonon behavior of the DGDR in hot nuclei confirms the existence of its building block (the hot GDR), where the quantal effects are mostly washed out. It has been shown within the PDM [20,21] that the GDR persists up to rather high temperature $T \sim 6$ MeV in agreement with the Brink hypothesis [31]. There is however another interpretation of the saturation of the width of the hot GDR that is related to the disappearance of the GDR at high temperature due to its exceedingly large width [32,33]. Therefore, an experimental observation of the DGDR in hot nuclei predicted in the present work would be decisive to confirm the existence of the GDR at high temperatures and to give the final solution to this puzzle.

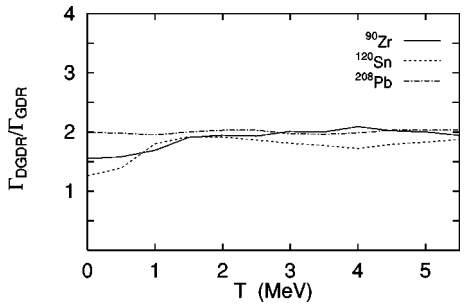

FIG. 5. The ratio between the DGDR and GDR widths as a function of temperatures.

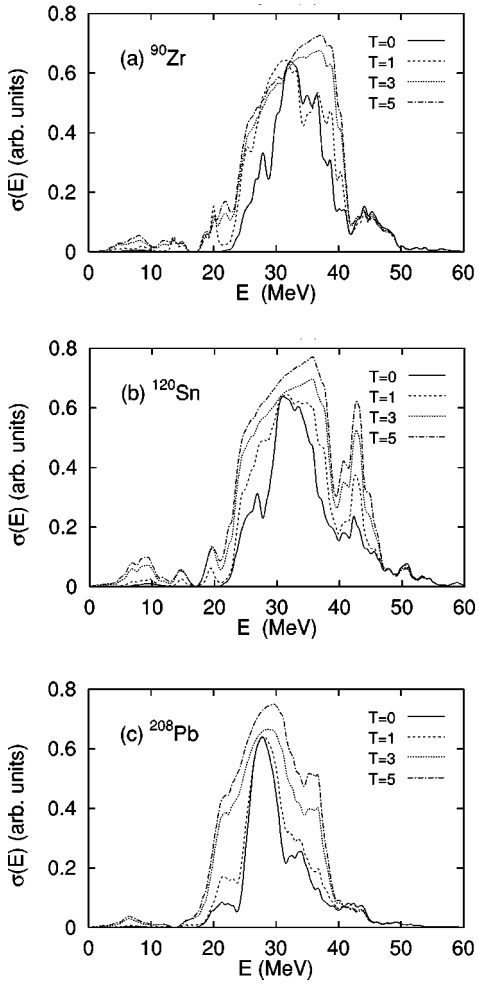

FIG. 6. Photoabsorption cross sections of the DGDR at several temperatures. The values of temperature are given in MeV.

The sharp increase of the DGDR width at low T and its saturation at high T shown in Figs. 3 and 4 lead to a sharp increase and saturation of the photoabsorption cross section in the DGDR region as shown in Fig. 6. Accordingly, the value σ_2 of the IPACS within the DGDR region between 22 MeV and 60 MeV also increases and saturates with increasing temperature. As a result, the enhancement of the IPACS $\sigma_2(T)$ as compared to its harmonic value σ_2^{har} at $T = 0$ increases with T and saturates at high T. In Fig. 7 the ratio

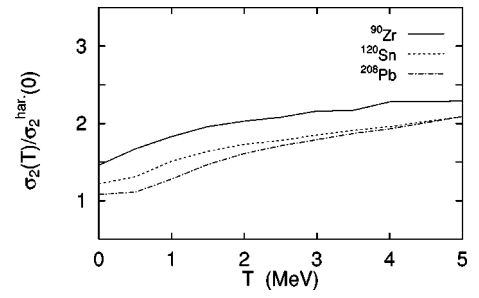

FIG. 7. The ratio between the value $\sigma_2(T)$ of the integrated photoabsorption cross section of DGDR and its harmonic value $\sigma_2^{\mathrm{har}}(T=0)$ as a function of temperature T.

$\sigma_2(T)/\sigma_2^{\rm har}(0)$ is plotted as a function of temperature. Already at $T=1$ MeV an enhancement factor of around 1.8 for ^{90}Zr, 1.5 for ^{120}Sn, and 1.3 for ^{208}Pb is seen for the IPACS of DGDR as compared to its harmonic value at $T=0$. Thus, the present analysis indicates a possibility that the enhancement of DGDR excitation cross section can be brought about if the DGDR is built on the hot GDR.

IV. CONCLUSIONS

We have proposed a simple yet microscopic approach to the DGDR. The present approach is based on the PDM, which has been successfully developed and applied to describe the damping of the hot GDR [18–21]. This approach allows the inclusion of the coupling of collective phonons generating the GDRs to the field of incoherent nucleon pairs. The natural extension to nonzero temperature is attained by making use of the double-time Green's function method. A closed set of coupled equations for the damping of the DGDR has been obtained and the analytical expressions for the width and energy shift of the DGDR have been derived. Using the same set of parameters previously selected for the description of the hot GDR, we have extensively applied this approach to calculate the width, energy, and strength function of the DGDR at zero as well as nonzero temperatures in ^{90}Zr, ^{120}Sn, and ^{208}Pb. The results of the numerical analysis allow us to draw the following conclusions.

(i) The anharmonic effect on the energy of the DGDR is rather small, which does not exceed 2% as compared to its value in the harmonic limit. The anharmonic effect on the width is more noticeable, confirming its quantal nature due to coupling of harmonic phonon oscillation to ph configurations at $T=0$. The effect is stronger in open shell nuclei such as ^{120}Sn, while it is rather small in double-magic nuclei such as ^{208}Pb. In ^{90}Zr, and ^{208}Pb the DGDR width is in a range between $\sqrt{2}\Gamma_{\rm GDR}$ and $2\Gamma_{\rm GDR}$, while in ^{120}Sn it is even smaller than $\sqrt{2}\Gamma_{\rm GDR}$ with $\Gamma_{\rm GDR}$ being the GDR width. The results of calculations are found in reasonable agreement with the experimental systematic for the width and energy of the DGDR in the region of mass number under consideration.

(ii) The anharmonic effect shows up more clearly in the DGDR strength function and, in particular, in the photoabsorption cross section. The IPACS within the energy interval from a value above the IVGQR (22 MeV) to 60 MeV is found enhanced by 46% in ^{90}Zr, 22% in ^{120}Sn, and 8% in ^{208}Pb as compared to the value in the harmonic limit. In our opinion this enhancement is directly related to the experimentally observed enhancement in the electromagnetic excitation cross section as compared to the theoretical estimations within the independent phonon picture.

(iii) At $T\neq 0$ the coupling to pp and hh configurations is open, which leads to a sharp increase of the DGDR width at low temperature and its saturation at $T>3$ MeV. The saturated values of the DGDR width are found to be around 21 MeV in ^{90}Zr, 24 MeV in ^{120}Sn, and 22.5 MeV in ^{208}Pb at $T\sim 5$ MeV. The DGDR shape changes drastically at low T but almost ceases to change at $T\geqslant 3$ MeV. We have also found that the harmonicity in the DGDR width is restored in open shell nuclei starting from $T\geqslant 1.5$ MeV due to the decrease of the quantal effect with increasing T. An experimental observation of the DGDR in hot nuclei is highly desirable to confirm the persistence of the GDR itself at high temperatures on the one hand, and the additional mechanism for the enhancement in the excitation cross section of the (hot) DGDR on the other hand.

In order to maintain the transparency of the argument utilizing our simple model, we have neglected in the present study a number of corrections such as the effect of higher-order graphs (e.g., three-phonon graphs), including the higher-order of boson operators in the boson mapping of the Pauli-correction graphs, coupling to continuum, etc. We also left out entirely the nonlinearity of the external field. The latter has been shown to be important to increase the integrated electromagnetic excitation cross section in the DGDR region [11,12]. It is our hope that inclusion of these effects in our approach will receive due attention in forthcoming studies.

ACKNOWLEDGMENTS

Numerical calculations were carried out by a 64-bit Alpha AXP work-station running Digital UNIX (OSF/1) at the Computer Science Laboratory of RIKEN. The authors thank G. Bertsch for turning their attention to Ref. [29].

[1] N. Frascaria, Nucl. Phys. **A583**, 63 (1995); Ph. Chomaz and N. Frascaria, Phys. Rep. **252**, 275 (1995).
[2] S. Mordechai *et al.*, Phys. Rev. Lett. **61**, 531 (1988).
[3] H. Emling, Prog. Part. Nucl. Phys. **33**, 629 (1994).
[4] K. Boretzky *et al.*, Phys. Lett. B **384**, 30 (1996).
[5] N. Frazier, B. A. Brown, and V. Zelevinsky, Phys. Rev. C **54**, 1665 (1996).
[6] Ph. Chomaz *et al.*, Z. Phys. A **319**, 167 (1984); Ph. Chomaz and N. Van Giai, Phys. Lett. B **282**, 13 (1992).
[7] S. Nishizaki and J. Wambach, Phys. Lett. B **349**, 7 (1995).
[8] S. Nishizaki and J. Wambach, Phys. Rev. C **57**, 1515 (1998).
[9] V. G. Soloviev, *Theory of Atomic Nuclei – Quasiparticles and Phonons* (IOP, Bristol, 1992).
[10] V. Yu. Ponomarev *et al.*, Phys. Rev. Lett. **72**, 1168 (1994); Z. Phys. A **356**, 251 (1996).
[11] E. G. Lanza *et al.*, Nucl. Phys. **A613**, 445 (1997).
[12] E. G. Lanza *et al.*, Nucl. Phys. **A636**, 452 (1998).
[13] H. Kurasawa and T. Suzuki, Nucl. Phys. **A597**, 374 (1996).
[14] N. Dinh Dang, A. Arima, V. G. Soloviev, and S. Yamaji, Phys. Rev. C **56**, 1350 (1997).
[15] J. J. Gaardhøje, Annu. Rev. Nucl. Part. Sci. **42**, 483 (1992).
[16] G. Enders *et al.*, Phys. Rev. Lett. **69**, 249 (1992).
[17] H. J. Hofmann *et al.*, Nucl. Phys. **A571**, 301 (1994).
[18] N. Dinh Dang and A. Arima, Phys. Rev. Lett. **80**, 4145 (1998).
[19] N. Dinh Dang and A. Arima, Nucl. Phys. **A636**, 443 (1998).
[20] N. Dinh Dang, K. Tanabe, and A. Arima, Phys. Rev. C **58**, 3374 (1998).
[21] N. Dinh Dang, K. Tanabe, and A. Arima, Nucl. Phys. **A645**, 536 (1999).

[22] G. Bertsch, P. F. Bortignon, and R. A. Broglia, Rev. Mod. Phys. **55**, 287 (1983).
[23] N. Dinh Dang and F. Sakata, Phys. Rev. C **55**, 2872 (1997).
[24] D. M. Brink, Nucl. Phys. **4**, 215 (1957); A. V. Ignatyuk and I. N. Mikhailov, Yad. Fiz. **33**, 919 (1981) [Sov. J. Nucl. Phys. **33**, 483 (1981)]; K. Neergard, Phys. Lett. **110B**, 7 (1982); P. Ring *et al.*, Nucl. Phys. **A419**, 261 (1984).
[25] N. N. Bogolyubov and S. Tyablikov, Sov. Phys. Dokl. **4**, 6 (1959).
[26] D. N. Zubarev, Usp. Fiz. Nauk. **71**, 71 (1960) [Sov. Phys. Usp. **3**, 320 (1960)]; *Nonequilibrium Statistical Thermodynamics* (Plenum, New York, 1974).
[27] M. Hage-Hassan and M. Lambert, Nucl. Phys. **A188**, 545 (1972).
[28] T. Aumann, P. F. Bortigon, and H. Emling, Annu. Rev. Nucl. Part. Sci. **48**, 351 (1998).
[29] G. F. Bertsch and H. Feldmeier, Phys. Rev. C **56**, 839 (1997).
[30] C. F. von Weizsäcker, Z. Phys. **88**, 612 (1934); E. J. Williams, Phys. Rev. **45**, 729 (1934).
[31] D. M. Brink, Ph.D. Thesis, Oxford University, 1955.
[32] K. Yoshida *et al.*, Phys. Lett. B **245**, 7 (1990).
[33] P. Chomaz, M. Di Toro, and A. Smerzi, Nucl. Phys. **A563**, 509 (1993); A. Bonasera *et al.*, *ibid.* **A569**, 215c (1994); V. Baran *et al.*, *ibid.* **A599**, 29c (1996).